Composite Structures 185 (2018) 549–560

Contents lists available at ScienceDirect

Composite Structures

journal homepage: www.elsevier.com/locate/compstruct

Geometric optimisation and compression design of natural fibre composite structural channel sections

M.R. Bambach

School of Civil Engineering, The University of Sydney, NSW 2006, Australia

ARTICLE INFO

Keywords:
Natural fibre composites
Flax
Jute
Hemp
Channels
Compression
Design

ABSTRACT

Public concerns about the environment, climate change, energy consumption and greenhouse gas emissions have placed increasing demands for the use of sustainable materials in the built environment. Natural fibres such as flax, jute and hemp have recently been considered for fibre-resin composites, with a major motivation for their implementation being their notable sustainability attributes. However, many studies have noted the relatively modest mechanical properties of natural fibre composites. Despite this, a recent paper by the author demonstrated that the compression strength of flat plates and plain channel sections may be suitable for light structural applications. This paper presents the geometric optimisation of channel sections via the inclusion of complex web, flange-edge and flange-interior stiffeners. It is demonstrated that the inclusion of geometric stiffeners restricts the development of local buckling, creating less slender channel sections with greater compression strength. Compression strengths are compared with steel and timber wall stud strengths and shown to be suitable for residential building applications. The combined plain channel and stiffened channel experimental data covers a broad range of section slenderness values, and design models are developed to predict their compression strength.

1. Introduction

Recent decades have seen substantial interest in the use of natural fibres in composite materials, where these fibres may be combined with thermoset or thermoplastic polymers to create natural fibre composites, which have been particularly identified for their sustainability attributes. Favourable sustainability properties of natural fibres such as flax, jute and hemp include: renewable resource; carbon sink; short growth cycle time (eg the sow to harvest cycle for flax is 100 days); low herbicide requirements due to rapid growth; low energy production; recyclable; biodegradable; and low hazard manufacturing and composite handling and working [1–7].

Much of the previous research has focused on the materials aspects, including fibre processing techniques, composite fabrication methodologies, matrix materials and their effects on the mechanical properties [8–13]. Most studies have demonstrated that natural fibre composites have comparably low intrinsic mechanical properties [2–13], and as a result, applications have thus far been limited to semi-structural or non-structural applications [14–22]. In a previous study, the author undertook an experimental program to characterise the intrinsic structural compression behaviour of natural fibre composites [23]. To establish the basic characteristics, the two fundamental components of flat plates and plain channel sections were considered, wherein a plain channel section consists of flat plate elements (web and flanges). These experiments demonstrated that the buckling and post-buckling responses were stable, the ultimate condition was reached in a stable and predictable manner, and failure ensued in a gradual and ductile process; characteristics that show promise for the use of natural fibre composite sections in light structural applications.

Many decades of research on thin-walled structures consisting of metals and plastics have demonstrated that compression buckling may be delayed with the use of discrete stiffeners placed in the zones of local buckling susceptibility. In this paper, the utility of complex stiffeners in natural fibre channel sections is studied, with the aim of optimising their compression strength. The stiffener design draws on the implementation of complex stiffeners in thin steel channel sections, particularly those used in the residential stud wall market. The overall dimensions of the channels also reflect such application, with a particular research question of the study being: could load bearing residential stud walls be manufactured from natural fibre composites? The results of the previous [23] and present study are used to develop a design procedure capable of predicting their compressive strength with reasonable accuracy.

E-mail address: mike.bambach@sydney.edu.au.

https://doi.org/10.1016/j.compstruct.2017.11.065
Received 13 September 2017; Received in revised form 7 November 2017; Accepted 21 November 2017
Available online 22 November 2017

2. Methods

2.1. Materials

Three different natural fibres were investigated in the present study; flax, jute and hemp. The flax and jute fabrics were commercially produced for fibre-resin composite fabrications by Composites Evolution; Biotex Flax 400 g/m^2 2 × 2 Twill weave and Biotex Jute 400 g/m^2 2 × 2 Twill weave. Nominal density, tensile strength and modulus values for the flax were; 1.5 g/cm^3, 500 MPa and 50GPa, and for the jute were; 1.46 g/cm^3, 400 MPa and 40GPa. The hemp fabric was not produced specifically for fibre-resin composite applications, however was recommended as the most appropriate fabric for working with resins by the manufacturer, and was a plain weave 287 g/m^2 pure unbleached hemp fabric with density 1.48 g/cm^3. The commercial bulk laminating epoxy resin Kinetix R240 with H126 (fast) hardener was used for all composite fabrications, with density 1.1 g/cm^3 and measured (neat) compression ultimate stress of 105.3 MPa, tension ultimate stress of 33.1 MPa and tension ultimate strain of 0.8% [23]. The channels were fabricated with a hand layup technique whereby each layer of fabric was wetted out with resin using a paint brush and roller. The fabrics were laid over a mandrel and held under a full vacuum during a cure time of a minimum of 5 h in a constant temperature room at 23 °C. Fibre volume fractions were calculated using the mass of fabric prior to fabrication, the mass of composite after fabrication, and the constituent densities.

2.2. Channel specimens

Flax, jute and hemp fibre-resin composite channels were fabricated with nominal geometries of web depth 100 mm, flange width 50 mm and 300 mm length. A length of three times the web depth was chosen since webs (stiffened elements) are known to nominally buckle in square half-wavelengths, and having three half-wavelengths of buckle minimises end effects. The channel lengths were short enough so as to preclude column member lateral-torsional buckling, such that the pure section capacity was established. The preclusion of column member lateral-torsional buckling was observed from the previous channel tests of length 300 m [23], and confirmed by the results observed in the present tests. Two different channel thicknesses were fabricated for each of the different fibre types; 4 and 6 fibre layers for the flax and jute channels, and 6 and 9 fibre layers for the hemp channels (in order to create hemp sections with similar fibre content to the flax and jute sections).

In the previous study [23] plain channel sections were tested, consisting of flat web and flange elements (Fig. 1a). Optimisation of the channel section geometry was considered by adding flange edge stiffeners, and additionally; one intermediate web stiffener (Fig. 1b and c), two intermediate web stiffeners (Fig. 1d and e), and two intermediate web stiffeners with one intermediate flange stiffener (Fig. 1f and g). For each web/flange stiffener arrangement, two different sized flange edge stiffeners were used. For all configurations (Fig. 1b–g) the smaller thickness was tested (4 layers of flax and jute and 6 layers of hemp), and for the configuration of two intermediate web stiffeners with one intermediate flange stiffener (Fig. 1f and g) the larger thickness was additionally tested (6 layers of flax and jute and 9 layers of hemp). The different stiffener configurations were fabricated by fixing 12 mm diameter half-rounds to the mandrel at specific locations, the mandrel being two 50 mm × 50 mm steel square hollow (SHS) sections with external corner radius of 6 mm. An example mandrel and resulting channel section is exemplified in Fig. 2. A split mandrel was required to facilitate extraction of the mandrel after curing. It is noted that 2 mm shim was placed between the SHS mandrel members to assist extraction, thus the nominal channel internal web depth was 102 mm. For the specimens with two intermediate web stiffeners, the rounded corners of the SHS resulted in a small central stiffener, as some fabric and epoxy was drawn into this space (Fig. 2a). This was an unintended artefact of the use of a split mandrel. The stiffeners were centrally located for all elements with one stiffener, and located at the quarter points for elements with two stiffeners (Fig. 2b). The channels were fabricated with approximate length 650 mm, then following curing were trimmed and cut into two 300 mm specimens using a standard powered circular drop saw with a timber cutting blade. The flange edge stiffeners were fabricated with approximate length of 40 mm, then following curing were trimmed to nominal dimensions of 20 mm or 30 mm using a high speed rotary tool (Dremel brand), with a carbide cutting wheel. The measured channel geometries are tabulated in Table 1. Exemplar channel specimens are shown in Fig. 3.

2.3. Channel section tests

The channels were tested in pure compression between fixed load platens. In order to reduce possible end effects such as eccentric loading or stress concentrations resulting from the channel ends not being completely flat and/or parallel, prior to testing 2 mm thick steel end plates were bonded to both ends of the channels using fast cure Araldite K219 epoxy. This resulted in the channel ends being essentially fixed ended, since end rotations were precluded. This method has been used and validated previously by the author [23,24]. Additionally, the channels were seated on a spherical bearing which when unlocked allowed free rotations in all directions. The test procedure involved placing the channel on the unlocked spherical bearing and applying a small load, then locking the spherical bearing such that rotations were then restrained. The restraint condition was thereby fixed end restraints. Four displacement transducers were located around the channels to measure the out-of-plane buckling deformations, including two on the web at the mid-length and quarter length, and one on each flange at the mid-length. The channels were loaded in displacement control at a speed of 0.5 mm/min.

In the previous tests [23], compression and tension material tests of the neat epoxy resin and fabricated fibre-resin materials were undertaken in accordance with ISO 604 [25] and ISO 527 [26], respectively. As the same constituent materials and fabrication procedures were used in the present study, these material values are nominally valid for the present channels also.

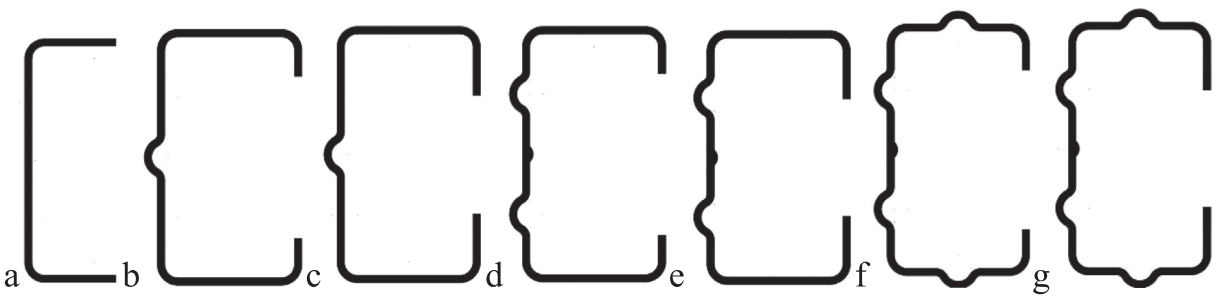

Fig. 1. Channel section geometries; a) plain (unstiffened) from [23], b) to g) stiffened (present study).

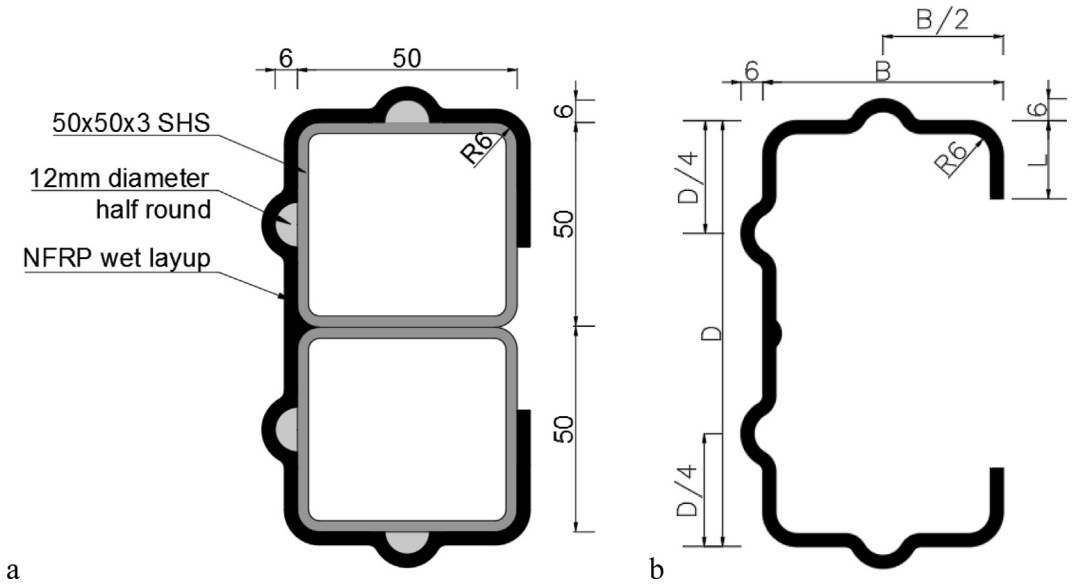

Fig. 2. Channel fabrication; a) exemplar fabrication mandrel, b) resulting channel section (B, D, L are outside dimensions).

2.4. Channel stub tests

In order to further characterise the material behaviour, short stubs of length 20 mm were cut from the thickest specimens (6 layers of flax and jute and 9 layers of hemp) during the trimming process, and tested in exactly the same manner as described above for the channel section tests. This allows for the characterisation of the section compressive strength when local buckling is precluded (since the specimen is too short to develop local buckling deformations).

2.5. Wall stud tests

In order for direct comparisons to be made between the natural fibre channel sections and typical structural members used in residential stud wall framing, steel and timber studs were also tested. For the steel studs, two different commercially produced stud wall framing members were tested, including one each of load bearing and non-load bearing (with respect to building gravity loads) studs. Both studs were manufactured by Rondo and were channel sections with a nominal web depth of 92 mm, flange width of 33 mm, and with flange edge stiffeners and two internal web stiffeners. The non-load bearing stud had thickness 0.55 mm, while the load bearing stud had thickness 1.15 mm, and both were cold-formed from nominal yield stress 300 MPa steel. For the timber studs a solid rectangular section of dimension 70 × 35 mm typically used for light or non-load bearing applications, and a solid rectangular section of dimension 90 × 45 mm typically used for load bearing applications, were tested. The timber material was commercially produced machine graded pine of structural grade 10 (MGP10), with a nominal characteristic strength of 16 MPa. All wall studs were tested with a length of 300 mm. One of each type of steel stud was tested, while four of each type of timber stud was tested and the minimum strength taken (since the timber contained knots and other imperfections along its length).

3. Results

3.1. Channel section tests

The fabrication technique generated consistent fibre volume fractions, and for all specimens the mean and standard deviations of the fibre volume fractions were; 42.1% and 0.9% for flax, 39.3% and 1.1% for jute and 34.8% and 1.9% for hemp, respectively. The slightly lower fibre volume fraction for hemp resulted from the more open weave in the hemp fabric. It is noted that the fibre volume fractions were estimated from the fibre mass fractions and the nominal fibre densities. Since it is possible that the fibres compressed slightly under the vacuum as a result of containing a lumen core, the fibre density may have increased slightly during fabrication, thus the calculated fibre volume fractions may be considered as upper bound estimates.

The channel compression test results are summarised in Table 1. The channels typically demonstrated a similar response to the previous channel tests [23], including a linear-elastic response followed by buckling, stable post-buckling, attainment of the ultimate load and then stable unloading. Attainment of the ultimate load was stable, i.e. in no cases was an unstable brittle fracture mode characterised by sudden failure and loss of load carrying capacity evident. Exemplar axial force – axial displacement plots with photographs of the specimens at ultimate are provided in Fig. 4a–c. Axial force – axial displacement plots of the strongest specimens of each material are shown in Fig. 4d. The channels tests were continued until the load reduced to at least 80% of the ultimate value, and the response demonstrated a very stable, gradual unloading mechanism.

A detailed depiction of the typical loading and post-ultimate unloading is shown in Fig. 5 for a flax specimen, including measurements from displacement transducers which were located at approximately the point of maximum buckling deformation in both the web and flange (being the mid-height since the channel buckled in a single half-wave). Initially the response is linear-elastic (zone 1 in Fig. 5), until the first bifurcation point which results from the initiation of local buckling. For the specimen shown, the web element buckles first as evidenced by the appearance of web transverse deformation, followed by buckling of the flange at a slightly higher load. The buckling deformations grow slowly at first, however after reaching approximately 1 mm grow rapidly. As the buckling deformations grow, the buckled regions increase in size and these regions become less effective in carrying axial load, thereby decreasing the section stiffness as the axial load redistributes into the unbuckled regions (zone 2). The axial stress continues to increase in the unbuckled regions, until it reaches the onset of matrix damage at which time the material begins to soften, and shortly thereafter the matrix fails (point 3) and the section begins to unload. During unloading the buckling deformations continue to grow (zone 4), and a point is reached where a fracture occurs in one flange edge stiffener (point 5), and then in the other flange edge stiffener (point 6). However, these fractures are highly localised and do not destabilise the section, such that the section

Table 1
Natural fibre composite channel section dimensions and test results (dimensions refer to Fig. 2, P refers to predicted values, f refers to stresses, F refers to loads, λ is the slenderness, E_c is the compression elastic modulus, A refers to area) (WS is web stiffener, SL is shorter length flange edge stiffener, LL is longer length flange edge stiffener and FS is internal flange stiffener).

Fibre	Section type	Layers	Fibre weight (g/m^2)	D (mm)	B (mm)	L (mm)	t (mm)	A_{net} (mm^2)	E_c (MPa)	f_{mf} (MPa)	f_{buckle} (MPa)	λ	$F_{ultimate}$ (kN)	$f_{buckleP}$ web (MPa)	$f_{buckleP}$ flange (MPa)	$f_{buckleP}$ lip (MPa)	A_{effP} (mm^2)	A_{effP}/A_{net}	$F_{ultimateP}$ (kN)	$F_{ultimate}/F_{ultimateP}$
Jute	1WS, SL	4	1600	110.2	57.4	18.4	3.4	829	3523	51.3	18.2	1.68	29.3	36.6	24.6	195	620	0.75	31.8	0.92
Jute	1WS, LL	4	1600	110.1	57.5	27.4	3.4	890	3523	51.3	19.4	1.62	32.7	36.6	25.1	49	629	0.71	32.3	1.01
Jute	2WS, SL	4	1600	112.1	57.2	17.8	3.4	860	3523	51.3	16.2	1.78	26.6	6.2	24.3	224	455	0.53	23.3	1.14
Jute	2WS, LL	4	1600	111.9	57.1	27.6	3.4	925	3523	51.3	16.5	1.76	28.0	6.2	25.1	48	465	0.50	23.8	1.17
Jute	2WS, 1FS, SL	4	1600	111.7	57.3	18.3	3.4	922	3523	51.3	16.3	1.78	29.3	6.1	24.6	200	499	0.54	25.6	1.15
Jute	2WS, 1FS, LL	4	1600	111.5	57.0	28.0	3.4	985	3523	51.3	16.3	1.77	35.8	6.1	24.8	46	505	0.51	25.9	1.38
Jute	2WS, 1FS, SL	6	2400	114.1	61.2	18.2	4.9	1359	3523	51.3	21.0	1.56	51.6	16.3	40.3	616	1037	0.76	53.2	0.97
Jute	2WS, 1FS, LL	6	2400	113.0	60.9	28.9	4.9	1455	3523	51.3	19.5	1.62	59.7	16.4	47.1	101	1045	0.72	53.6	1.11
Flax	1WS, SL	4	1600	109.2	56.9	17.9	3.3	796	4199	61.5	18.7	1.81	28.2	42.3	28.0	240	583	0.73	35.9	0.78
Flax	1WS, LL	4	1600	109.0	57.1	27.9	3.3	862	4199	61.5	19.9	1.76	30.8	42.5	28.2	51	592	0.69	36.4	0.84
Flax	2WS, SL	4	1600	111.2	56.6	18.1	3.3	831	4199	61.5	18.1	1.85	28.2	6.9	28.6	229	430	0.52	26.4	1.07
Flax	2WS, LL	4	1600	111.1	56.8	28.9	3.3	903	4199	61.5	20.6	1.73	33.3	6.9	27.3	46	433	0.48	26.6	1.25
Flax	2WS, 1FS, SL	4	1600	109.9	56.9	19.9	3.3	898	4199	61.5	20.7	1.72	32.5	6.8	29.6	158	477	0.53	29.3	1.11
Flax	2WS, 1FS, LL	4	1600	110.3	56.8	28.2	3.3	953	4199	61.5	21.1	1.71	33.5	6.8	28.0	50	474	0.50	29.2	1.15
Flax	2WS, 1FS, SL	6	2400	113.2	60.1	18.4	4.8	1319	4199	61.5	26.3	1.53	59.4	18.8	49.2	650	995	0.75	61.2	0.97
Flax	2WS, 1FS, LL	6	2400	113.1	60.1	28.1	4.8	1412	4199	61.5	23.7	1.61	69.2	18.7	55.6	125	1003	0.71	61.7	1.12
Hemp	1WS, SL	6	1722	111.2	58.6	18.2	4.0	977	2649	60.7	16.0	1.95	28.0	35.8	22.2	245	651	0.67	39.5	0.71
Hemp	1WS, LL	6	1722	111.6	58.9	28.1	4.0	1060	2649	60.7	18.7	1.80	42.9	35.5	22.7	50	658	0.62	40.0	1.07
Hemp	2WS, SL	6	1722	112.6	58.2	18.4	4.0	1017	2649	60.7	15.1	2.00	29.5	7.4	22.8	233	506	0.50	30.7	0.96
Hemp	2WS, LL	6	1722	112.9	58.1	27.2	4.0	1088	2649	60.7	19.4	1.77	48.4	7.4	23.5	56	513	0.47	31.1	1.55
Hemp	2WS, 1FS, SL	6	1722	112.1	58.5	17.9	4.0	1086	2649	60.7	20.8	1.71	47.4	7.3	22.1	264	545	0.50	33.1	1.43
Hemp	2WS, 1FS, LL	6	1722	112.2	58.6	27.6	4.0	1165	2649	60.7	25.0	1.56	48.7	7.3	23.1	53	557	0.48	33.8	1.44
Hemp	2WS, 1FS, SL	9	2583	114.9	61.9	18.1	5.3	1475	2649	60.7	25.6	1.54	60.6	15.4	31.5	625	967	0.66	58.7	1.03
Hemp	2WS, 1FS, LL	9	2583	114.5	61.7	28.4	5.3	1580	2649	60.7	24.1	1.59	68.9	15.4	35.6	99	1007	0.64	61.2	1.13
																			Mean:	1.10
																			COV:	0.19

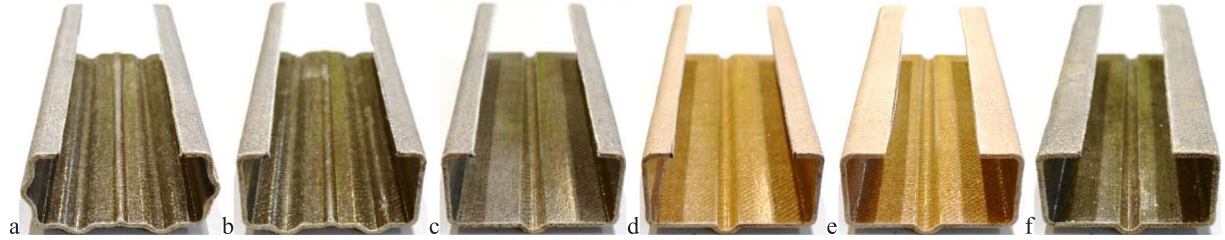

Fig. 3. Exemplar channel sections: a) flax (Fig. 1f); b) flax (Fig. 1d); c) flax (Fig. 1b); d) jute (Fig. 1b); e) jute (Fig. 1c); and f) hemp (Fig. 1c) (channels a to e consist of 4 layers, channel f consists of 6 layers).

continues to unload in a stable, gradual manner. As with the previous tests [23], the section buckling load was quantified using the change in stiffness method [27], using the intersection of the pre-buckled and post-buckled stiffness tangents (Fig.5), and converted to the section buckling stress by dividing by the net cross-section area (f_{buckle} and A_{net} in Table 1).

Generally speaking, the behaviour of all the channels sections were similar to that described above, however the flange tended to buckle before the web when a flange intermediate stiffener was not present, while fractures in the flange edge stiffener did not always occur. Most channels deformed in a single half-wave of buckling, while the flanges buckled either inwards or outwards. This is different to the plain channels [23], where most specimens buckled in two or three half-waves. This is likely related to the fact that the stiffened channels in the present study were substantially less slender than the unstiffened channels.

3.2. Channel stub tests

The results of the 20 mm length channel stub tests (Fig. 6) provide further information regarding the section behaviour described above. Since local buckling of the section was precluded by their length, the response was dominated by matrix behaviour. Initially the response was linear-elastic, then as matrix damage initiated the material began to soften, thus the axial stress – axial displacement curve bifurcated (i.e. the section stiffness reduced). Matrix damage then continued until matrix failure, identified as the ultimate stress. Matrix damage initiated at; 52.1 MPa (flax), 40.3 MPa (jute) and 42.1 MPa (hemp). Matrix failure occurred at; 61.5 MPa (flax), 51.3 MPa (jute) and 60.7 MPa (hemp). Since all section buckling stresses were well below the matrix damage initiation values (between 15.1 MPa and 26.3 MPa in Table 1), it can be confirmed that the first bifurcation point on the axial force – axial displacement channel section plots for the 300 mm length sections corresponded to local buckling rather than the onset of matrix damage.

It is interesting to note that the compression ultimate stresses (f_{uC}) determined in accordance with ISO 604 [25] (as detailed in [23]) are somewhat lower than those determined using the 20 mm channel stubs; 38.5 MPa (flax), 40.2 MPa (jute) and 33.9 MPa (hemp). These were derived from compression coupons with dimensions 10 × 10 mm and thickness between 3.4 mm and 3.6 mm (4 layers of flax and jute and 6 layers of hemp). This difference likely results from the fact that in the channel stubs matrix failure initiation is localised in regions, rather than the entire cross-section undergoing matrix failure simultaneously as occurs in the small 10 × 10 mm flat specimens. This might result from the fact that the stubs are not flat elements like the compression coupons. The rounded corners, for example, might provide more resistance to fibre delamination and matrix failure than the flat areas (Fig. 7a). As such, compared with the compression coupons, the corners might undergo matrix failure at a substantially higher stress, and might also provide support to the adjacent flats allowing those areas to undergo matrix failure at a higher stress. Photos of matrix failure in exemplar stub and 300 mm length sections are shown in Fig. 7. Since the compression moduli were determined in the purely elastic range prior to matrix damage and failure [25], this issue should not affect the moduli values. However as discussed further in Section 4, for the purposes of analyses of channel sections the full section matrix failure stress (f_{mf}) is a useful value, thus it may be useful to perform compression material tests both on small samples in accordance with [25], and on short full section stubs. Accordingly, the full material properties are summarised in Table 2.

3.3. Section optimisation

With regards to section optimisation, the maximum compression strengths in Table 1 are summarised in Fig. 8 (including the results of plain channels from [23]), including maximum compression stresses (Fig. 8a) and maximum compression forces (Fig. 8b). It is demonstrated in this figure that the addition of stiffeners generally increases the compression strength (Fig. 8b), and the selection of fibre type, thickness and stiffener arrangement can result in channel compression strengths ranging anywhere between 2.1 kN and 69.2 kN. However, the addition of stiffeners also increases the cross-section area, thus part of this increase is due simply to the addition of material. Consideration of the maximum average stress, i.e. the compression strength divided by the net cross-section area, better demonstrates the effect of the addition of stiffeners on the structural efficiency (Fig. 8a). Efficient stiffeners will delay the onset of local buckling, thus allowing the section to reach a larger maximum average stress. Comparison of the sections with flange edge stiffeners and a single web stiffener with the equal thickness plain sections demonstrates this well, where the maximum average stress increases up to 2.3 times. While there was a large strength difference between channels with and without stiffeners, the differences between different stiffener arrangements were less pronounced. Generally speaking for the flax and jute sections, using two web stiffeners instead of one slightly decreased the maximum average stress since the web buckled at a lower stress, however also adding a flange intermediate stiffener slightly increased the maximum average stress again since the flange buckled at a higher stress. The web with a single stiffener had a slightly better resistance to buckling than two stiffeners since the single stiffener was located precisely at the point of maximum local buckling deformation. While outside the scope of the present study, it is noted that the two web stiffener arrangement is frequently used in thin-walled steel members since when subjected to bending, this arrangement places a stiffener at the point of maximum compression buckling deformation (thus members that will be subjected to combined compression and bending tend to perform better with two web stiffeners). For all channel sections, increasing the flange edge stiffener length generally slightly increased the maximum average stress since the flange buckled at a higher stress, and increasing the thickness generally increased the maximum average stress since all elements buckled at a higher load.

It should be noted that only one specimen of each type was tested, and it is well known that thin sections undergoing local buckling are susceptible to imperfections, which may have resulted in small discrepancies from trends in buckling loads and strengths. Additionally, buckling and post-buckling are highly non-linear behaviours, thus small changes in one variable can result in large changes in response, and vice versa. It is also noted that the hemp channels displayed the reverse

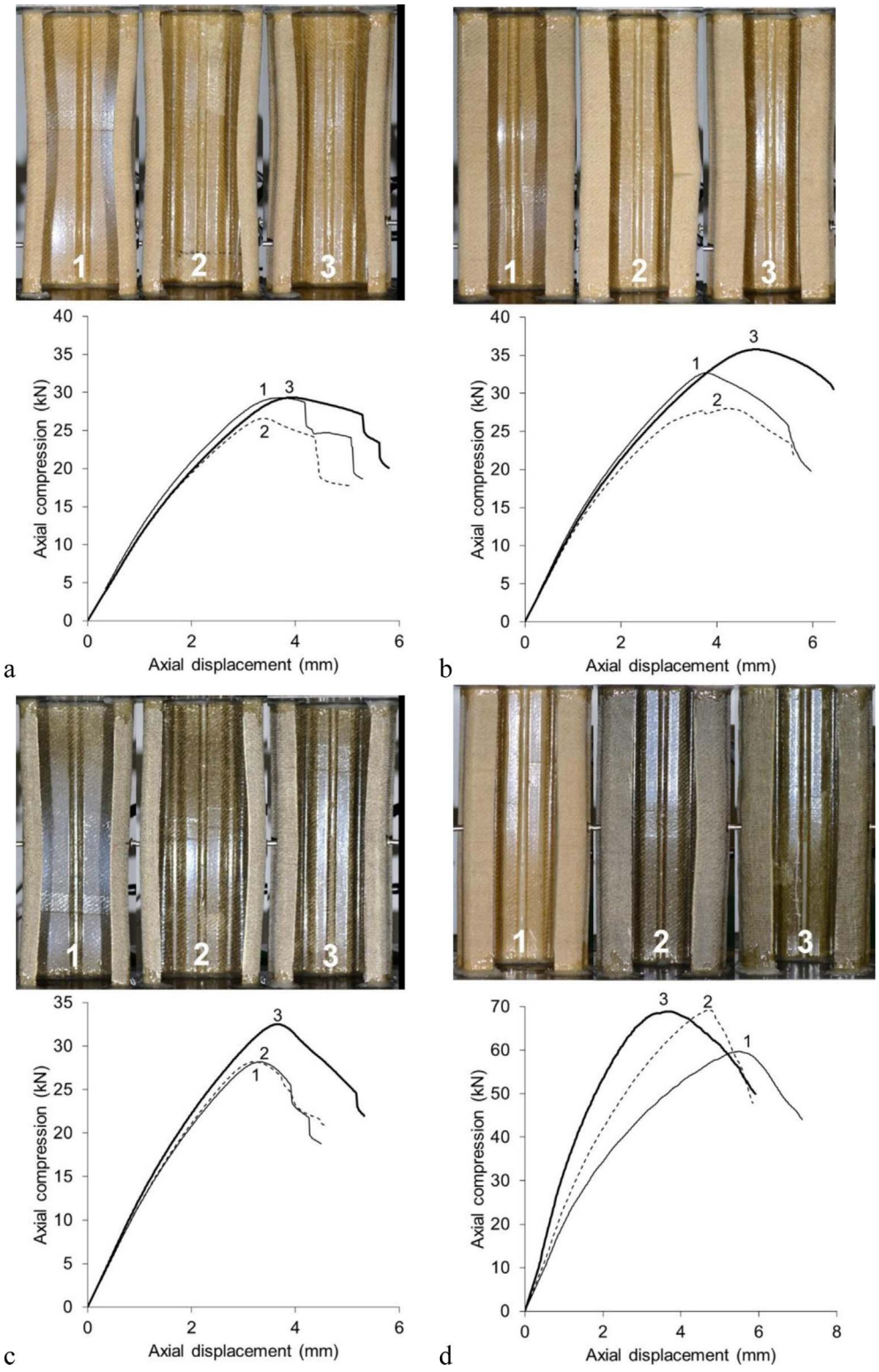

Fig. 4. Exemplar channel compression test results; a) jute 4 layers SL (1: 1WS, 2: 2WS, 3: 2WS and 1FS), b) jute 4 layers LL (1: 1WS, 2: 2WS, 3: 2WS and 1FS), c) flax 4 layers SL (1: 1WS, 2: 2WS, 3: 2WS and 1FS), d) 6 layers of flax and jute and 9 layers of hemp 2WS, 1FS and LL (1: jute, 2: flax, 3: hemp) (WS is web stiffener, SL is shorter length flange edge stiffener, LL is longer length flange edge stiffener and FS is internal flange stiffener).

trend to that noted above for the flax and jute webs, the reasons for which are unclear, however may be related to the fact that they were notably thicker than the flax and jute sections due to the extra layers required to achieve the same fibre mass (Table 1).

The hemp channels also displayed an unusual trend with regards to flange buckling, where the small change in flange edge stiffener length resulted in a large increase in strength (Fig. 8) for the flat flanges, however this did not occur for the flanges with an intermediate stiffener. The stabilising effect of a flange edge stiffener element (of any material) relates to its second moment of area, which is in turn relates to its length cubed, thus small changes in this length can lead to large effects. In the case of the hemp channels, it is likely that the longer edge stiffener was sufficient in stiffness to fully stabilise the flange, while the shorter stiffener was not. The addition of the flange intermediate stiffener likely also led to a fully stabilised flange, such that in this case the effect of the edge stiffener length became small again (since the flange was already stabilised). These effects might also relate to the larger thickness of the hemp channels, which were between 8% and 17%

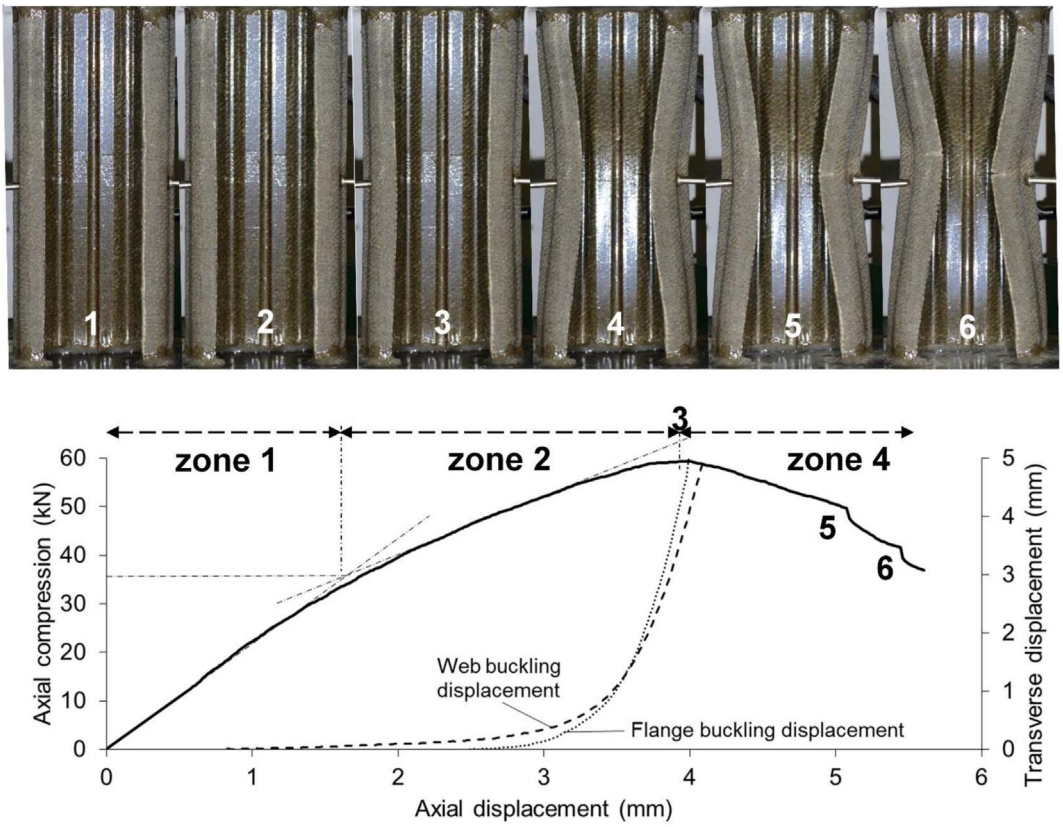

Fig. 5. Exemplar full compression test result for 6 layers of flax with two web stiffeners, one flange intermediate stiffener and shorter length flange edge stiffener.

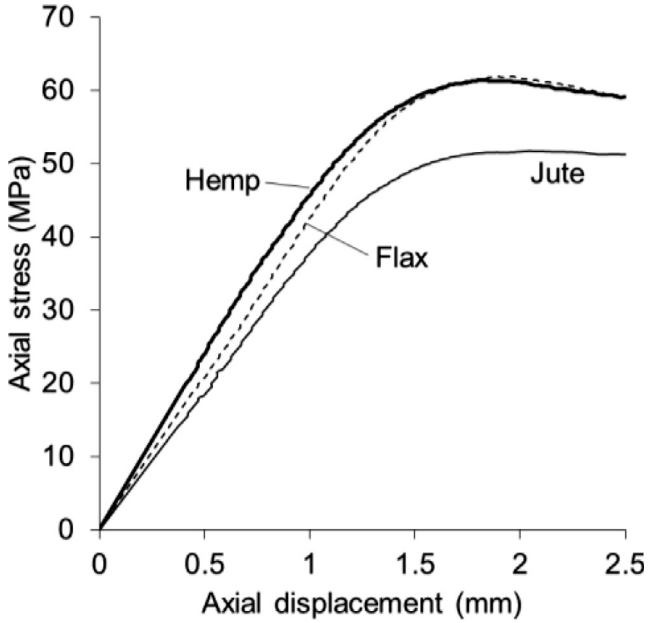

Fig. 6. Compression test results of 20 mm length channel stubs of 6 layers of flax and jute and 9 layers of hemp, with two web stiffeners, one flange intermediate stiffener and longer length flange edge stiffener.

thicker than the flax and jute channels with equivalent fibre mass. This resulted in the hemp channels being nominally less prone to local buckling than the equivalent flax and jute channels, while the hemp channels had lower fibre volume fractions. Less slender sections (of any material) are also more prone to small variations in local buckling stresses causing large variations in strength, since strength curves related to local buckling have much higher gradient as the slenderness decreases (as discussed further in Section 4).

With regards to overall optimisation of natural fibre composite channels, the thicker channels (2400 gsm) with flange and web stiffeners reached approximately 80% of the maximum stress of their respective 20 mm stubs, indicating that local buckling of the elements was still reducing their potential strength. It is difficult for a full length member to reach 100%, since out-of-plane geometric imperfections will typically result in out-of-plane displacements and some softening even when fully developed buckling is precluded. Nonetheless, there is possibly potential to improve the efficiency slightly more, either with more and/or larger stiffeners, and/or more fibre layers.

3.4. Wall stud tests

The results of the steel and timber wall stud tests are compared with the flax channels with 6 layers (the strongest natural fibre channel) and 4 layers in Fig. 9. The compression strengths of the non-load bearing and load bearing steel studs were 12.7 kN and 41.0 kN, and correspondingly for the timber studs were 57.7 kN and 106.8 kN, respectively. Considering the steel studs as a benchmark for the minimum compression strength required for stud walls, comparison with the results in Table 1 indicates that all of the stiffened channel sections would be suitable for use as non-load bearing wall studs, while all of the thicker (6 layers of flax and jute and 9 layers of hemp) stiffened channels would be suitable for load bearing walls. It is noted, however, that the natural fibre channels are substantially less stiff than the steel and timber studs, thus serviceability requirements would need to be considered (amongst other factors discussed further in Section 5).

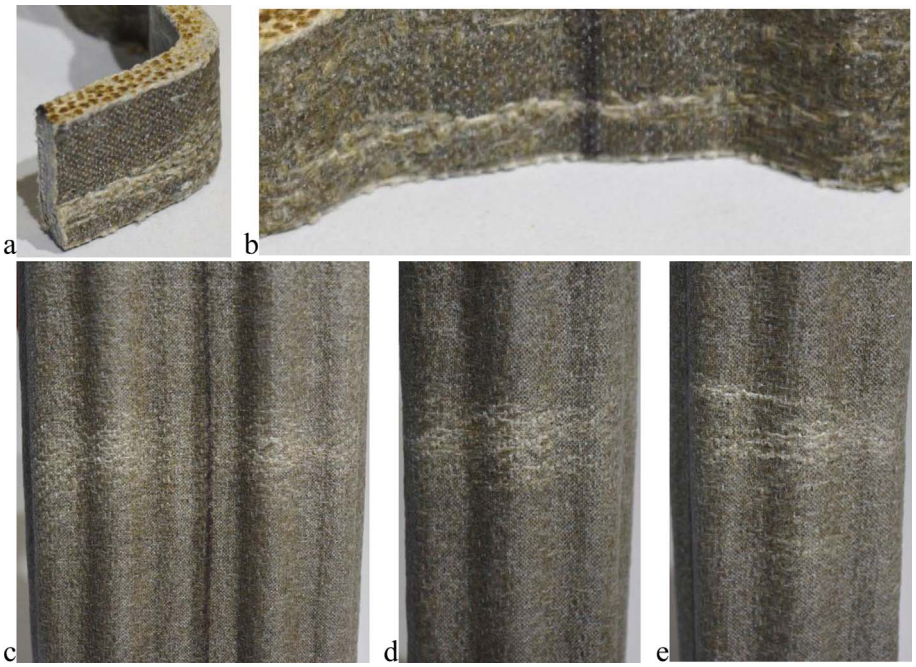

Fig. 7. Photographs of matrix failure in flax specimens; a) flange edge stiffener in 20 mm stub specimen, b) area between web stiffeners in 20 mm stub specimen, c) web of channel in Fig. 5, d) and e) flanges of channel in Fig. 5.

Table 2
Material properties of the natural fibre composites and the epoxy resin (neat) (T refers to tension, C refers to compression, f_{uC} and f_{uT} are the ultimate compression and tension stresses, respectively, according to material tests specified by [25,26], ε_{uT} is the failure strain in tension according to material tests specified by [26], f_{mf} is the full section matrix failure stress according to full channel section stub tests of length 20 mm).

	E_T (MPa)	f_{uT} (MPa)	ε_{uT} (%)	E_C (MPa)	f_{uC} (MPa)	f_{mf} (MPa)
Kinetix R240	4362	33.1	0.8	3588	105.3	–
Flax	6030	45.4	3.1	4199	38.5	61.5
Jute	5184	52.1	1.6	3523	40.2	51.3
Hemp	3826	35.3	1.8	2649	33.9	60.7

4. Design

4.1. Effective width mechanics model

The effective width mechanics model has been used internationally for many decades to design thin-walled steel structures undergoing compression buckling. The models' success results from the realistic depiction of the post-buckling mechanics of thin elements, wherein the assumption is made that the buckled regions become ineffective in carrying load, redistributing the axial load to the unbuckled regions, which resist the load until some limit stress is reached (e.g. the yield stress for steel). For the natural fibre composite channels in the present

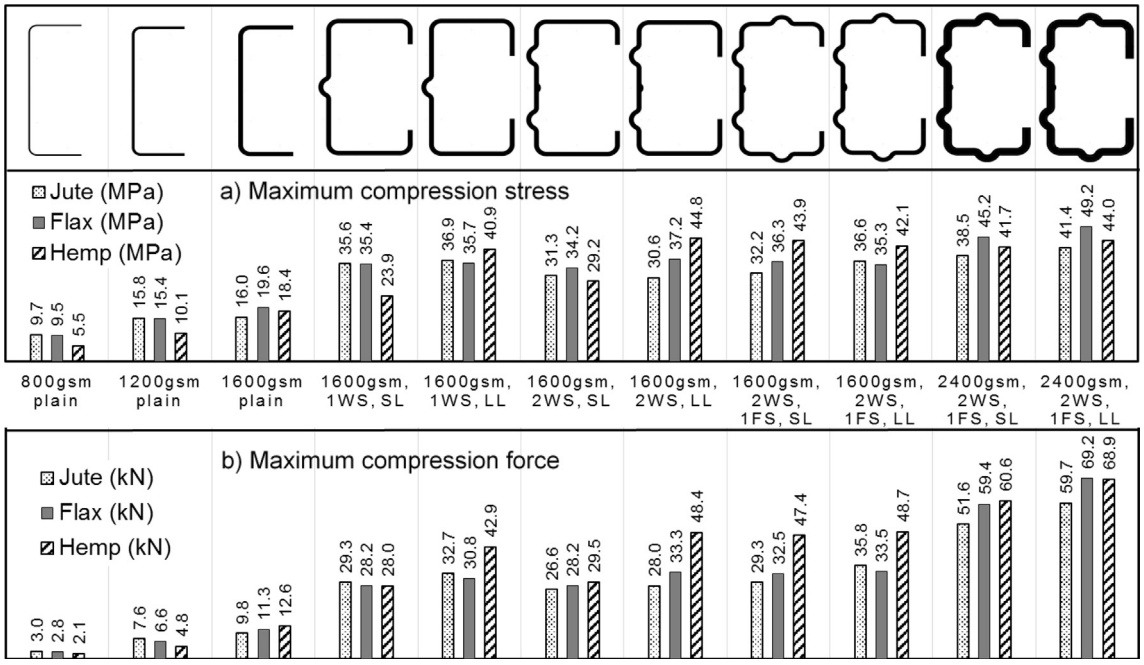

Fig. 8. Summary of compression tests in plain [23] and stiffened channels; a) maximum average compression stress (maximum force divided by the net cross-section area), b) maximum force (WS is web stiffener, SL is shorter length flange edge stiffener, LL is longer length flange edge stiffener and FS is internal flange stiffener) (fibre masses vary slightly for hemp, see Table 1 for exact values).

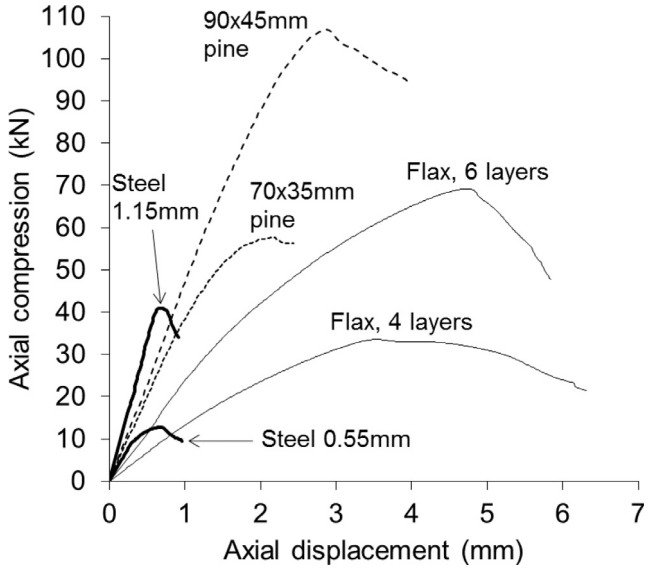

Fig. 9. Comparison of 300 mm length stud wall columns of steel Rondo studs, timber MGP10 pine studs and flax with two web stiffeners, one flange intermediate stiffener and longer length flange edge stiffener.

study the effective width concept is demonstrated in Fig. 10. The limit stress was taken as the measured full section matrix failure stress established from the 20 mm length channel stubs (f_{mf}, Table 2). The experimental effective area of the section at the limit state (A_{eff}) is given by Eq. (1), where $F_{ultimate}$ is the ultimate compression load in the test.

$$A_{eff} = \frac{F_{ultimate}}{f_{mf}} \tag{1}$$

For design purposes, the method requires a prediction of the buckling stress and an equation that relates the buckling stress to the effective width that ensues at the limit state (the strength equation). The strength equation is derived empirically from plate and/or section tests. The Winter strength Eq. (2) is used to calculate the post-buckling strength of thin steel sections. The previous natural fibre plain channel section strengths were shown to be slightly over-predicted by this equation [23]. Accordingly, an empirical modification was proposed given by Eq. (3), which provided a lower bound to the test results. In these equations the effectiveness factor (the ratio of the effective area to the net area of the section, ρ) is a function of the non-dimensionalised buckling stress (Eq. (4)), termed the section slenderness (λ), where f_{cr} is the buckling stress.

$$\rho = \frac{A_{eff}}{A} = \frac{1-\frac{0.22}{\lambda}}{\lambda} \leqslant 1 \tag{2}$$

$$\rho = \left(\frac{1-\frac{0.22}{\lambda}}{\lambda}\right)^{1.5} \leqslant 1 \tag{3}$$

$$\lambda = \sqrt{\left(\frac{f_{mf}}{f_{cr}}\right)} \tag{4}$$

Comparison of the present channel tests with the modified Winter Eq. (3), using the experimentally determined buckling stresses and effectiveness factors, indicated that the strength equation under-predicted the test results for less slender channels (Fig. 11a). A new strength equation for natural fibre composite channel sections was therefore empirically derived by determining a least-squares best-fit of all the channel data in a power format. The resulting equation is given by Eq. (5) and compares relatively well with the channel data (Fig. 11b), with an R^2 value of 0.83.

$$\rho = \frac{1.28}{\lambda^{1.5}} \leqslant 1 \tag{5}$$

4.2. Buckling

The design methodology requires an estimate of the buckling stress. The channels were fabricated with a biaxial [0,90] woven fabric and were therefore not strictly quasi-isotropic (given that ± 45 layers were not included). Nonetheless, for the purposes of the present loading case of pure compression resulting in buckling induced membrane strains in the two principle orthogonal directions, and without significant shear stresses nor shear buckling, an isotropic theory was considered potentially appropriate. Additionally, individual specimens had the same amount of fibre in the 0 and 90 directions, and since the elements were thin the through-thickness properties were not especially important. In the previous study [23] an isotropic buckling theory was found to provide reasonable estimates of the buckling stress, albeit over-predicting the experimental values, which was attributed to the theory not accounting for geometric and/or material imperfections. The theoretical buckling stress (f_{cr}) of flat thin isotropic plates is given by Eq. (6), where E is the elastic modulus, t is the plate thickness, b is the plate width, υ is Poisson's ratio and k is the elastic buckling coefficient.

$$f_{cr} = \frac{k\pi^2 E}{12(1-\upsilon^2)}\left(\frac{t}{b}\right)^2 \tag{6}$$

For plain channels, the elastic buckling coefficient (k) was 4 for the web and 0.43 for the flange, since these were flat elements. For the stiffened channels the calculation of the buckling coefficient is substantially more complex, and requires several geometric calculations. In keeping with the use of relevant design equations for thin-walled steel, the calculations for the buckling coefficients used in the Australian specification for cold-formed steel structures [28] were assessed for their utility for the channels. Many equations are involved in these

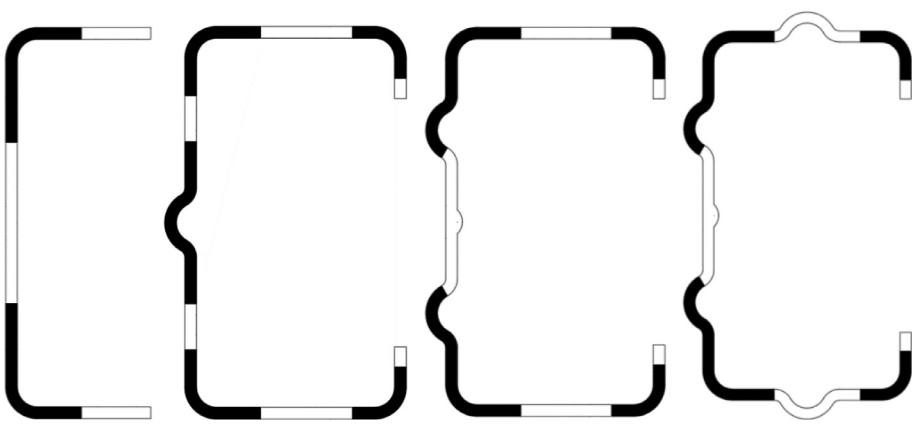

Fig. 10. Exemplar effective widths (black areas) of channel sections at the limit state.

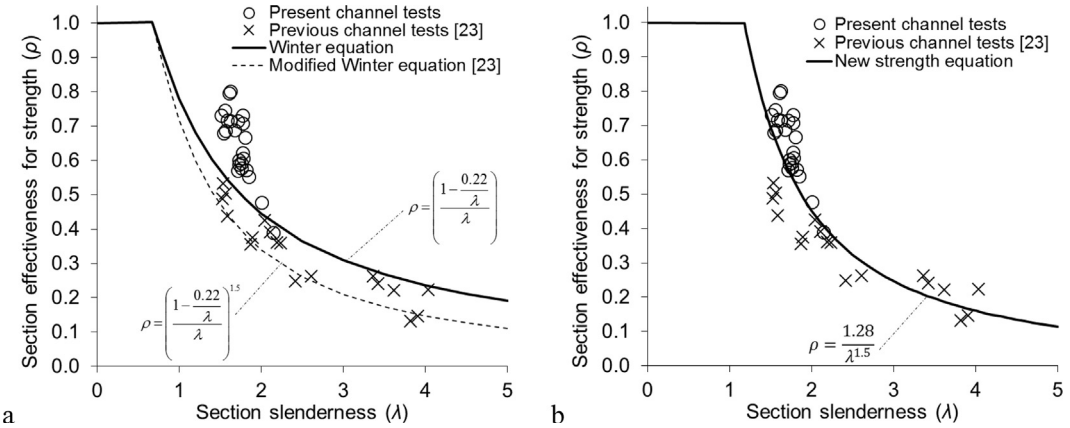

Fig. 11. Strength curves for natural fibre composite channels compared with test data (using experimental values of section effectiveness and slenderness), unstiffened [23] and stiffened channels.

calculations thus they are not reprinted herein, however fully worked example calculations are provided for the different channel geometries in the online supplementary material to this article. The buckling stress predictions using these procedures are summarised in Table 1. It is difficult to compare these values with the experimental values, since the method calculates buckling stresses for each individual element (web, flanges, flange edge stiffeners), while single 'section buckling' stresses were calculated from the channel tests. However, examination of the values confirms several trends evident in the experimental results, such as: the buckling stress of the web decreased with the addition of a second web stiffener; the buckling stress of the flange increased with increasing flange edge stiffener length; and the buckling stresses of all elements increased with thickness. While the different elements may buckle at different stresses, the net effect of one of more buckled elements reaching a certain buckling magnitude is a quantifiable bifurcation from section linear elasticity (Fig. 5). The exact relationship between these has not been precisely established (for steel nor for natural fibre channels).

4.3. Strength predictions

The element theoretical buckling stresses were used to calculate the element effective widths (Eqs. (4) and (5)), which were then summed to establish the design effective section area. Eq. (1) was then used to calculate the design compression strength. These values are tabulated in Table 1 and shown to compare relatively well with the experimental values, with a mean test/predicted ratio of 1.10 and coefficient of variation of 0.19. The large coefficient of variation is attributed more to the hemp channels than the flax and jute, where there was a substantial amount of variation between tested and predicted values for the hemp (between 0.71 and 1.55). This may be a result of larger imperfections resulting from the more open and imperfect weave in the hemp material, compared with the flax and jute weaves which were processed very precisely specifically for composites fabrication. Nonetheless for design purposes, such variability may be accounted for using capacity factors derived from a reliability analysis. Using the methodology outlined in [28] a capacity factor of 0.75 was derived for a reliability index of 3.0 (Fig. 12). This indicates that design ultimate strengths calculated using the above technique should be reduced by 25% for design purposes, which provides an acceptably low probability of the design load exceeding the ultimate strength. It should be noted that in this analysis several parameters used nominal values since large datasets of natural fibre composite channel sections are not available.

5. Discussion

While the mechanical properties of natural fibre composites are relatively modest, the buckling and post-buckling responses were shown to be stable, the ultimate condition was reached in a stable and predictable manner, and the failure ensued in a gradual and ductile process. These stable compression characteristics imply an inherent suitability for structural applications. The relatively modest compression strengths lend themselves to light structural applications, potentially in the residential and light commercial markets. Typical Australian domestic stud wall column design loads were calculated previously [23], and shown to vary between around 5 kN and 15 kN per stud column. These results indicate that the natural fibre composite channels developed in the present study are well suited to such application, with strengths between 27 kN and 69 kN. Of course these strengths are section strengths, and full length columns may have strengths reduced by column buckling, however given that the columns could likely be braced with noggins and claddings this should not result in substantial reductions in capacity (however this requires further research).

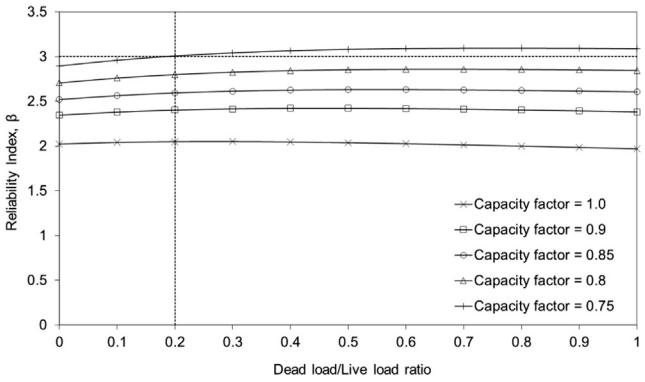

Fig. 12. Natural fibre composite channel section reliability analysis according to [28] for the effective width design method (Eqs. (4)(6)) compared with test data (Table 1).

Comparison with commercial residential steel wall stud columns in the present study confirms the suitability of the natural fibre composite channels for this application, wherein non-load bearing and load bearing steel studs had capacities of 13 kN and 41 kN. The timber studs had higher strengths (58 kN and 107 kN), however such members need to be substantially over-designed due to the large capacity variations resulting from imperfections in the timber (knots, grain orientation, wanes, splits, etc) and the machine grading process. The maximum natural fibre composite channel strength achieved in the present study was 69 kN, and considering the channels could be placed back-to-back (or fabricated as an I-section), the combined capacity of 138 kN (14 tons) indicates they are potentially suitable for a wide range of light structural applications. Clearly, there are many factors that would need

to be addressed before natural fibre composites could be introduced into buildings, for example; fatigue-related matrix damage, column buckling, other loading types, connections, fire performance, environmental exposure and durability, etc., which were outside the scope of the present study. Serviceability limitations would need to be carefully considered, since the natural fibre composite channels were much less stiff than the timber and steel counterparts. As is typical in structural design, there will be circumstances in which serviceability limits control the design rather than strength limits.

Another attribute that potentially indicates the suitability of natural fibre channels for light structural applications is the predictable nature of their compression strength. Within the limitations of the small sample in the present study, the effective width mechanics model showed reasonable accuracy for estimating the section strength. With regards to the elastic buckling stress estimation, there were differences between theoretical and observed values, and the isotropic theory used could potentially be unsuitable for other loading conditions (for example in bending when shear develops). While many theories exist for the buckling of layered anisotropic composites, these would need to be coupled with geometric theories capable of accounting for the complex geometries required for efficient structural sections, such as complex edge and internal stiffeners. The computational demand of such procedures might lend themselves to numerical solutions, such as finite strip and finite element procedures. Nonetheless, these can easily be accommodated in design approaches in the manner currently done with thin steel structures [28], where the designer is permitted to use any rational theoretical or numerical procedure to calculate the buckling stress, and these values are then used with a suitable strength equation to predict the capacity. With regards to the natural fibre composite strength equation developed in the present study, good correlation was observed between experimental buckling stresses and strengths. However, further research might reveal different fibre and matrix layouts and load cases require different strength equations to be developed, or other issues such as the fact that natural fibres are highly impacted by growth conditions, and the fibre-matrix bond is typically poor and subject to treatment, since the constituents are polar and no-polar, respectively. Additionally, the design capacity factor may require modification as more experimental data becomes available. In summary, the present study has demonstrated the utility of the effective width design approach, however buckling solutions, strength equations and capacity factors should be developed further in the future as more research becomes available.

It also is worthy to note that natural fibre composites may be mechanically worked without the potential risks associated with synthetic fibres. In the present study high speed timber cutting tools were used with only the typical PPE recommended for working with power tools, which provides a substantial advantage for natural fibres over their synthetic counterparts, both for industrial manufacturing and building site workability.

It is also noted that in the present paper channel section stubs of length 20 mm were introduced as a potential measure to provide further information regarding the ultimate compression stress of a natural fibre channel section, in addition to those properties obtained from compression coupons such as per ISO 604 [25]. The selected length of 20 mm was somewhat arbitrary, in that it was simply the shortest length that could be conveniently cut from the full channel length. The utility of these compression strength values was demonstrated in the present paper, where the compression strength of the 300 mm channel section in which local buckling can occur, can be directly compared with the compression strength of the channel section when local buckling is precluded (the 20 mm stub). Despite the fact the 20 mm stubs do not conform to any standardised procedure, such values are also particularly useful in the application of the effective width method. However, some differences were noted between the compression stresses thus obtained and those from compression coupons, which warrants further study.

With regards to fibre weave, there was substantially more variation noted in the strength results of the hemp channels, which was attributed to the more open and imperfect weave in the hemp fabric compared with the flax and jute fabrics (which were processed fabrics produced specifically for composites fabrication). The higher variability in the hemp strength results potentially indicates that less uniform fabrics will produce less uniform composites, and will correspondingly produce less uniform strength results.

6. Conclusions

Increasing awareness of environmental concerns is leading a drive towards more sustainable structural materials for the built environment. The present study has further demonstrated the reliable and predictable mechanical behaviour of natural fibre composite structures of flax, jute and hemp in pure compression. The introduction of complex geometric stiffeners into natural fibre channel sections, in the same vein as they have been implemented into thin steel channel sections, has demonstrated substantial structural efficiencies. The geometrically optimised natural fibre composite channels have been demonstrated to have compression capacities suitable for residential wall stud applications, identifying them as a potentially viable alternative to traditional building materials in such application, and potentially other light structural applications. The utility of the effective width method to predict their strength has been demonstrated, however the procedures could be improved over time as more research becomes available.

Appendix A. Supplementary data

Supplementary data associated with this article can be found, in the online version, at http://dx.doi.org/10.1016/j.compstruct.2017.11.065.

References

[1] Summerscales J, Dissanayake NPJ, Virk AS, Hall W. A review of bast fibres and their composites. Part 1 – fibres as reinforcements. Composites A 2010;41:1329–35.
[2] Summerscales J, Dissanayake NPJ, Virk AS, Hall W. A review of bast fibres and their composites. Part 2 – composites. Composites A 2010;41:1336–44.
[3] Ku H, Wang H, Pattarachaiyakoop N, Trada M. A review on the tensile properties of natural fibre reinforced polymer composites. Composites B 2011;42:856–73.
[4] Yan LB, Chouw N, Jayaraman K. Flax fiber and its composites – a review. Composites B 2014;56:296–317.
[5] Pickering KL, Efendy MGA, Le TM. A review of recent developments in natural fibre composites and their mechanical performance. Composites A 2016;83:98–112.
[6] Faruk O, Bledzki A, Fink H, Sain M. Biocomposites reinforced with natural fibres: 2000–2010. Prog Polym Sci 2012;37:1552–96.
[7] Dicker M, Duckworth P, Baker A, Francois G, Hazzard M. Green composites: a review of material attributes and complementary applications. Composites A 2014;56:280–9.
[8] Weclawski BT, Fan M, Hui D. Compressive behaviour of natural fibre composite. Composites B 2014;67:183–91.
[9] Costa FHMM, D'Almeida JRM. Effect of water absorption on the mechanical properties of sisal and jute fibre composites. Polym Plast Technol Eng 1999;38(5):1081–94.
[10] Hargitai H, Racz I, Anandjiwala RD. Development of hemp fiber reinforced polypropylene composites. J Therm Comp Mat 2008;21:165–74.
[11] Oksman K. High quality flax fibre composites manufactured by the resin transfer moulding process. J Reinf Plast Comp 2001;20(7):621–7.
[12] Van de Weyenberg I, Ivens J, De Coster A, Kino B, Baetens E, Verpoest. Influence of processing and chemical treatment of flax fibres on their composites. Comp Sci Tech 2003;63:1241–6.
[13] Lefeuvre A, Bourmaud A, Morvan C, Baley C. Elementary flax fibre tensile properties: correlation between stress-strain behaviour and fibre composition. Ind Crops Prod 2014;52:762–9.
[14] Dittenber D, GangRao H. Critical review of recent publications on use of natural composites in infrastructure. Composites A 2012;43:1419–29.
[15] Yan LB, Chouw N. Crashworthiness characteristics of flax fibre reinforced epoxy tubes for energy absorption application. Mat Des 2013;51:629–40.
[16] Yan LB, Chouw N. Behaviour and analytical modelling of natural flax fibre reinforced polymer tube encased coir fibre reinforced concrete composite column. J Comp Mater 2013;47(17):2133–48.
[17] Mak K, Fam A, McDougall C. Flexural behavior of sandwich panels with bio-FRP skins made of flax fibers and epoxidized pine-oil resin. J Compos Constr 2015;19(6):04015005.

[18] Duigou AL, Deux JM, Davies P, Baley C. PLLA/flax mat/balsa bio-sandwich manufacture and mechanical properties. Appl Compos Mater 2011;18:421–38.
[19] Uddin N, Kalyankar RR. Manufacturing and structural feasibility of natural fiber reinforced polymeric structural insulated panels for panelized construction. Int J Polym Sci 2011;96:35–49.
[20] Shah DU, Schubel PJ, Clifford MJ. Can flax replace E-glass in structural composites? A small wind turbine blade case study. Composites B 2013;52:172–81.
[21] Corradi S, Isidori T, Corradi M, Soleri F. Composite boat hulls with bamboo natural fibres. Int J Mater Prod Technol 2009;36(1):73–89.
[22] Alvarez-Valencia D, Dagher HJ, Lopez-Anido RA, Davids WG, Gardner DJ, Center AC. Behavior of natural-fiber/thermoplastic sheet piling. ACMA-composites and polycon conference, January 2009, Tampa, Florida, USA; 2009.
[23] Bambach MR. Compression strength of natural fibre composite plates and sections of flax, jute and hemp. Thin-Walled Struct 2017;119:103–13.
[24] Bambach MR. Axial capacity and crushing of thin-walled metal, fibre-epoxy and composite metal-fibre tubes. Thin-Walled Struct 2010;48(6):440–52.
[25] ISO 604:2002. Plastics – Determination of compressive properties.
[26] ISO 527-4:1997. Plastics – Determination of tensile properties. Part 4: Test conditions for isotropic and orthotropic fibre-reinforced plastic composites.
[27] Bambach MR. Photogrammetry measurements of buckling modes and interactions in channels with edge stiffened flanges. Thin-Walled Struct 2009;47(5):485–504.
[28] AS/NZS 4600:2005. Australian/New Zealand standard. Sydney: Cold-Formed Steel Structures, Standards Australia; 2005.